Bending and Torsional Fatigue of Nylon 66 Monofilaments

MARY TONEY and PETER SCHWARTZ

Fiber Science Program, Cornell University, Ithaca, New York 14853-4401

SYNOPSIS

Using newly developed test equipment, the fatigue behavior of nylon 66 monofilaments was studied under two loading conditions, pure bending or simple torsion. For each mode, results are expressed in terms of the measured decay in stiffness with numbers of cycles over a range of maximum applied strain levels. Fatigue lifetimes are presented in S–N format where the log number of cycles of fatigue for a 40% decay in stiffness (N) is plotted as a function of applied strain (S). The failure mechanism for these fibers in each fatigue mode reflects the morphology of semicrystalline-oriented synthetic fibers. In torsion, many longitudinal cracks form around the perimeter of a fiber as the result of cleavage of the relatively weak interfibrillar bonds in nylon 66. In bending, cracks form within kink band boundaries and grow at an oblique angle to the fiber axis. © 1992 John Wiley & Sons, Inc.

INTRODUCTION

In the past, attention has been focused on the use of oriented polymeric fibers as load bearing, structural elements in engineering applications, such as in marine ropes, industrial belts, and fiber-reinforced composites. The tensile fracture and fatigue behaviors of candidate materials are often studied because axial strength and stiffness are usually optimized during processing. In service, however, typical single-fiber deformations include bending, torsion, compression, and/or tension. Simulation of most actual service conditions is virtually impossible. In a given situation, however, one of the applied modes of deformation will presumably dominate the fiber response. Therefore, perhaps a better understanding of the behavior of synthetic fibers in service can be obtained by investigating the behavior of these materials in simple loadings *independent* of other modes. With this presumption, equipment was developed, as described elsewhere,[1] to independently test the bending and torsional fatigue behaviors of synthetic monofilaments.

Journal of Applied Polymer Science, Vol. 46, 2023–2032 (1992)
 CCC 0021-8995/92/112023-10

EXPERIMENTAL

Using the aforementioned test equipment,[1] a group of nylon 66 monofilaments was subjected to controlled cyclic applications of strain on each of the two machines, a torsional fatigue tester (TFT) and a bending fatigue tester (BFT). Each sample was allowed to progress in time to complete fracture, with the induced moment recorded during the course of the sample lifetime. Fatigue tests were performed at fixed frequency of 3 Hz under controlled atmospheric conditions of 21°C (±1°C) and 65% (±2%) relative humidity while varying the amplitude of the applied strain and level of molecular orientation. In each case, the deformation was applied in balanced cycles of positive and negative displacements.

The nylon 66 monofilaments were manufactured at the Albany International Research Company. The polymer chip source was a natural grade, DuPont Zytel 42, and the fibers were melt spun into a water quench with an in-line hot-air draw. The final product had an average diameter of 0.43 mm and one of two draw ratios; namely, 4.1× or 5.2×, subsequently referred to as low and high draw, respectively. Several classic laboratory tests were performed on the material for the purpose of physical characterization. Typical tensile stress–strain curves, shown in Figure

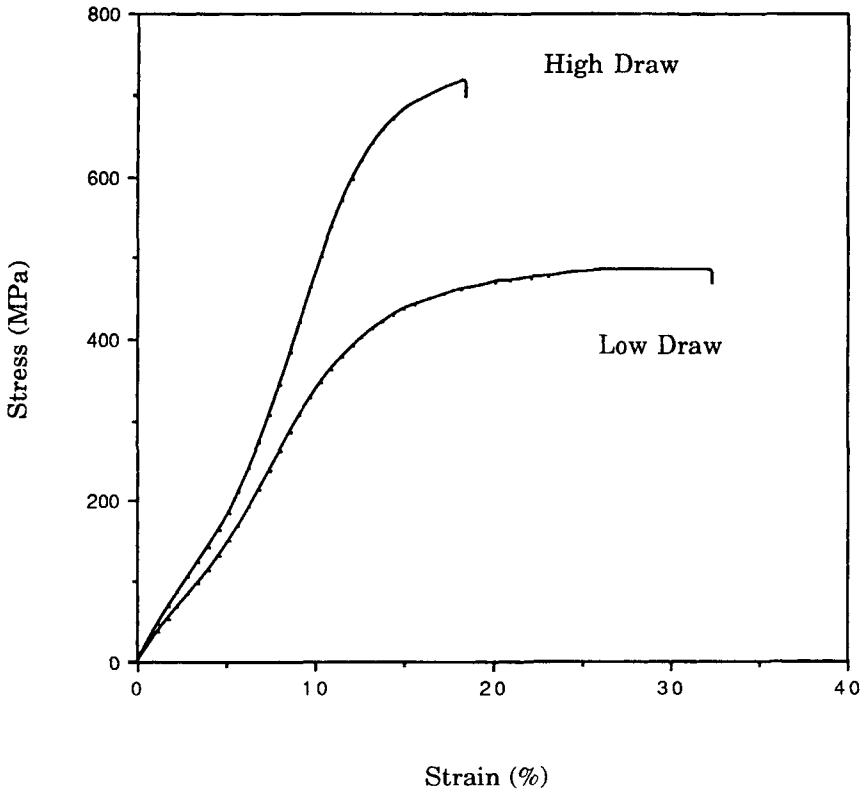

Figure 1 Typical stress–strain behavior for nylon 66 monofilaments.

1, were obtained with an Instron 1122 machine at a sample gauge length of 40 cm and a strain rate of 50% per minute. Quasi-static shear modulus values were obtained using the torsion pendulum technique.[2] Crystallinity values were deduced from relative heat of fusion values obtained with a Perkin-Elmer differential scanning calorimeter (DSC-4). A summary of the static physical properties for the fibers is presented in Table I where the mean values are followed by the coefficients of variation in parentheses. The high draw material has a greater initial tensile modulus than the low draw material, but the two exhibit essentially the same shear moduli and level of crystallinity.

Table I Monofilament Physical Properties

Draw Ratio	Tensile Modulus (GPa)	Shear Modulus (GPa)	Crystallinity (%)
Low	3.36 (3.4%)	0.50 (10.8%)	42.2 (1.0%)
High	4.47 (3.0%)	0.49 (6.1%)	43.3 (1.0%)

RESULTS AND DISCUSSION

Torsional Fatigue Tester

Using the TFT, samples of each draw ratio were carefully selected for roundness and uniformity (0.427 mm diameter) and subjected to repeated cycles of torsional displacement. In one cycle on the TFT, a sample is twisted first to the right and then to the left about a neutral position. The maximum applied displacement, $(d\phi/dz)_{max}$, for a given sample was at one of three twist levels; namely, ±0.38, ±0.47, or ±0.59 rad/mm. The corresponding maximum surface strain, γ_{max}, per cycle for the experimental fibers was ±8.1, ±10.0, or ±12.7% as

$$\gamma_{max} = r(d\phi/dz)_{max}$$

with r being the fiber radius. For a fiber in simple torsion, at a given radial position the strain is uniform along and around the fiber and has a maximum value at the surface of the fiber. For a given element away from the center of the filament, the shear strain alternates positive and negative with each cycle.

Although the applied displacement was assumed

to be pure torsion, a minimal amount of axial strain was present in each sample. The source of the axial load was twofold; first from a static load applied during mounting to aid in proper alignment of the sample in the grips (0.7 MPa) and, second, from the load induced in the twisted sample because of a restriction on sample foreshortening (measured to be less than 3 MPa). The level of axial stress therefore never exceeded 4 MPa and was thus deemed negligible as it was well within the elastic regime. Furthermore, as will be next discussed, the observed fracture topography was exclusively the result of critical torsional strains, not axial strains.

The load response of each sample was monitored throughout the lifetime of the sample, and the amplitude of the induced torque was seen to decay with numbers of cycles for each sample. In Figure 2, a typical load response as a function of numbers of cycles is shown for a nylon 66 sample at each of the three imposed levels of maximum surface strain per cycle. Here the load has been converted to torsional moment and normalized with respect to the first recorded moment for each sample. As would be expected, samples subjected to higher surface strains in a given test configuration show an earlier decay in load response. Although only three typical cases are shown in Figure 2, for all samples the relative moment decays with increasing numbers of cycles, typically reaching a plateau at about 30% of the initial value. The samples are visibly damaged at this point.

Plotting the data in the format used in Figure 2, the fatigue lifetime for each sample was defined arbitrarily as the number of cycles required to cause a decay in torsional moment from an initial value of 1.0 to a value of 0.6. This lifetime behavior is best represented in the form of an S-N curve as shown in Figure 3, where, for each sample, the log number of cycles shown to produce a 40% decay in relative torsional moment (N) is plotted against the maximum theoretical applied surface shear strain (S). A summary of the lifetime results is shown in Table II, where each value represents the average of at least five sample values. The data are well fit with a least-squares linear model on to semilog basis for a correlation coefficient of 0.93. There is no statistical difference ($\alpha = 0.01$) in the torsional fatigue lifetime between the low and the high draw material.

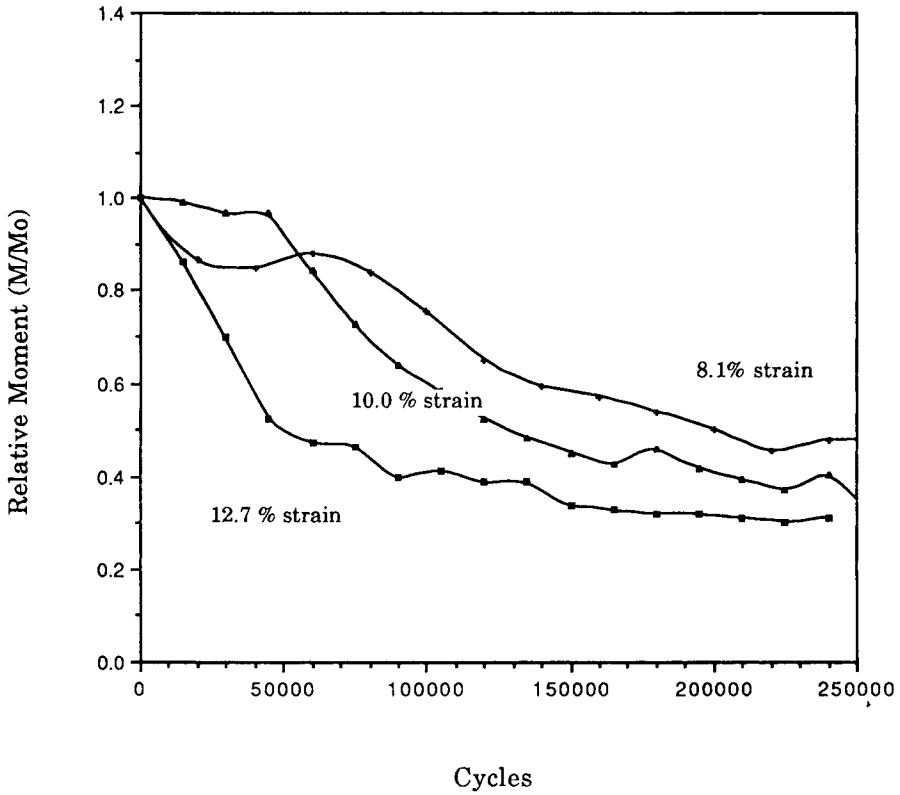

Figure 2 A typical response of nylon 66 monofilament to torsional fatigue at each of three different imposed levels of maximum surface strain per cycle.

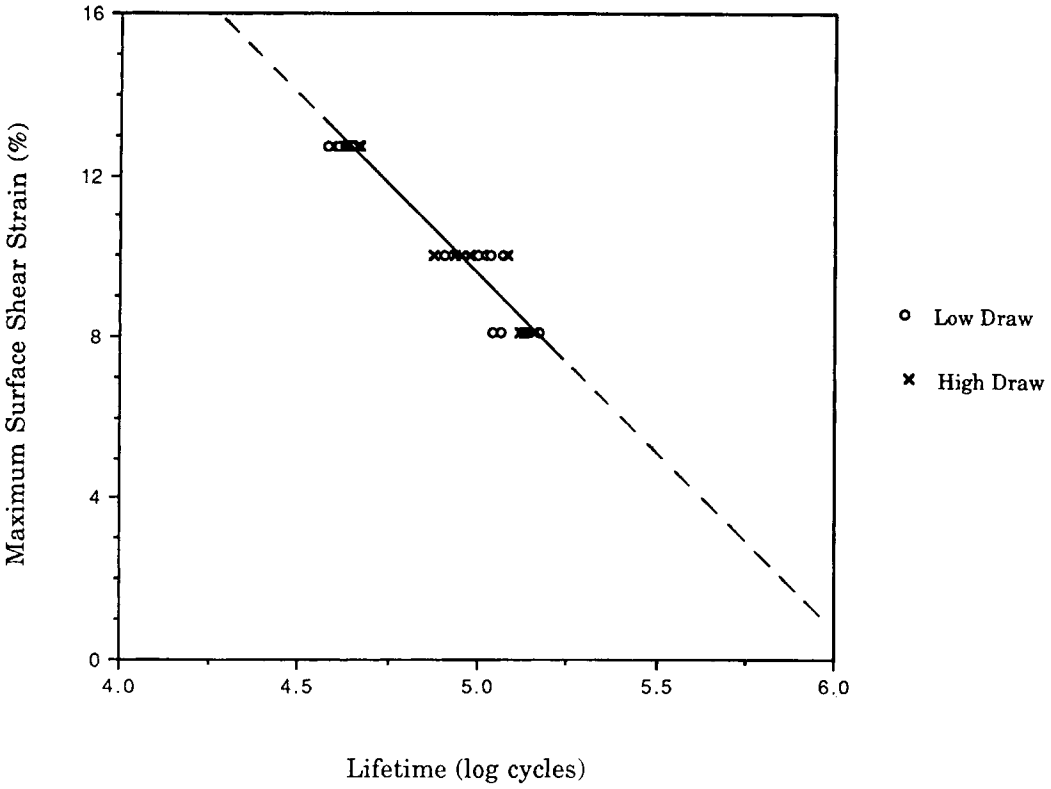

Figure 3 Torsional fatigue S–N lifetime for nylon 66 monofilament.

The decay in torsional stiffness and strength of these fibers is due to the formation of many longitudinal cracks, uniformly distributed around the fiber in damage zones. Photographs of several representative samples are shown in Figure 4. Polymer debris often accumulated at the surface edges of the cracks. The zone length of the fatigue cracks was usually on the order of 2–4 mm (or about one half to one fourth the sample gauge length), and the cracks were uniformly distributed about the perimeter of the fiber in these zones. Very few of the cracks ran the full length of the zone so that the multitude of short cracks sufficiently disrupted the material causing a reduction in strength and stiffness.

A limited experiment testing residual fiber strength with fatigue cycles was performed with the low draw material at the intermediate strain setting. Apparently, as represented in Figure 5, the fatigue cracks simply reduce the effective radius of the fiber by the average depth of the cracks. Since the torsional stiffness is proportional to the fourth power of the radius, and the strength is proportional to the square of the radius, an effective-area model yields an expected relative stiffness equal to the square of the relative strength. This is the case for these fibers, as shown in Table III.

The nature of the fatigue cracks resulting from torsional fatigue is the same for these monofilaments as has been observed for other oriented synthetic fibers subjected to torsional fatigue.[3,4] The cracks form along a weak boundary in the polymer structure. In this case of pure shear applied with respect

Table II Torsional Fatigue Lifetimes at 60% Relative Moment

Maximum Twist [rad/mm]	Surface Shear Strain	Low Draw Mean Cycles [Thousands] (CV)	High Draw Mean Cycles [Thousands] (CV)
0.38	0.081	128.7 (12.1%)	138.2 (4.0%)
0.47	0.100	102.7 (13.6%)	93.2 (18.2%)
0.59	0.127	40.3 (4.0%)	44.9 (4.4%)

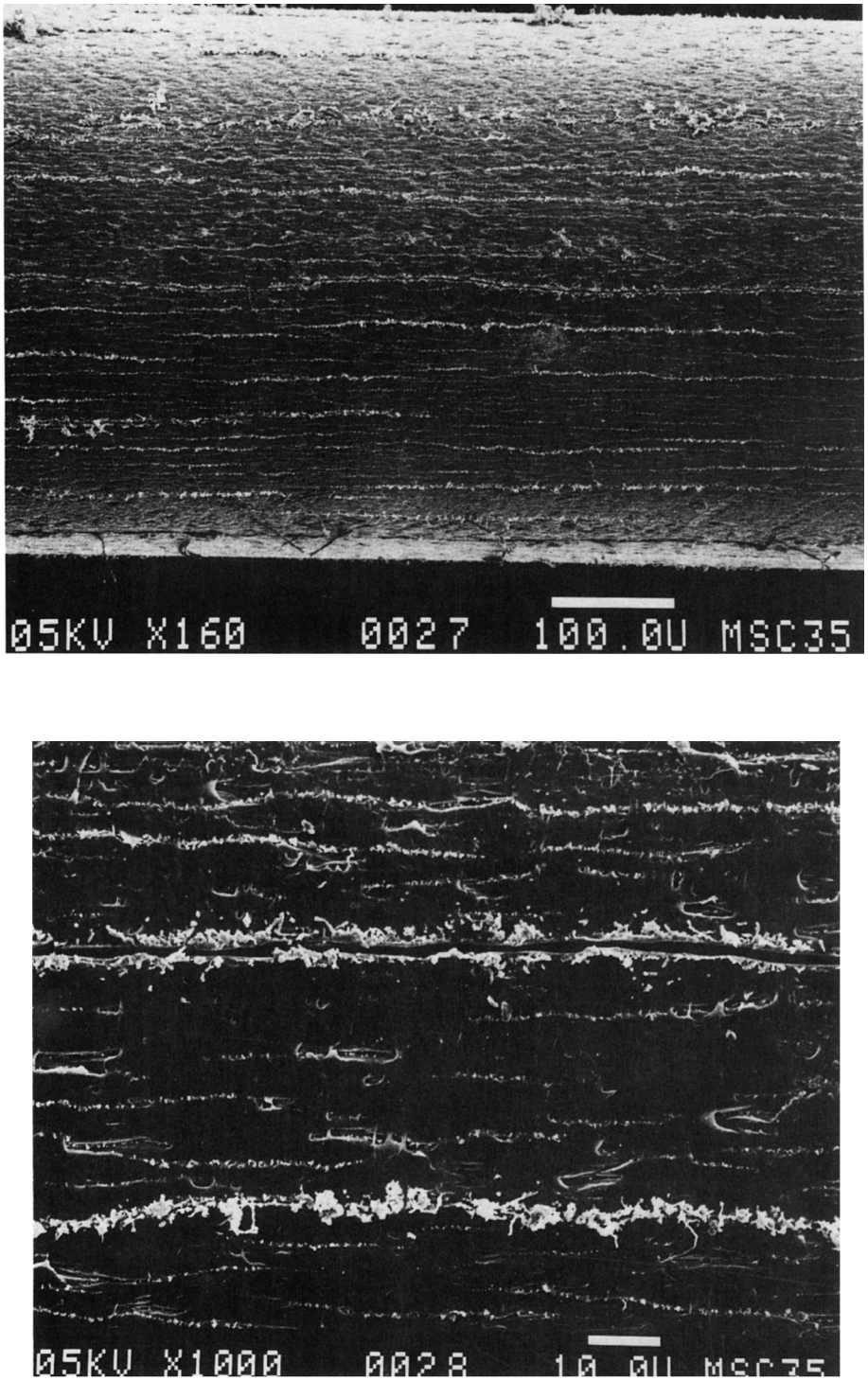

Figure 4 Typical crack formation in nylon 66 after torsional fatigue (↔ fiber axis).

to the fiber axis, the interfibrillar hydrogen bonds appear to be the weak link in the structure. Because the shear strain is a function of radial distance, the probability of crack formation is the same for any location about the fiber at a given radius. Therefore, many cracks would be expected to form uniformly about the fiber, beginning at the surface where the applied shear strain is the greatest. This has been observed for these fibers, as well as for the fibers in the earlier studies.

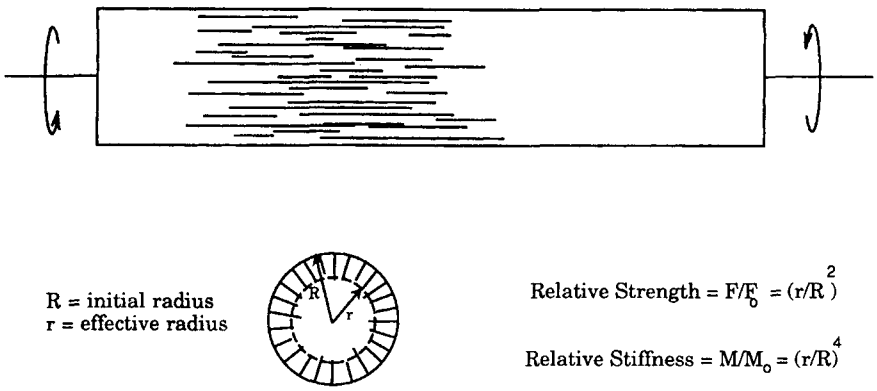

Figure 5 Model for fiber fatigued in torsion.

Bending Fatigue Tester

The bending fatigue behavior of the same group of nylon 66 monofilaments was assessed with the BFT equipment. This test equipment is unique in that a fiber is subjected to pure bending, that is, there are no extraneous effects from friction, wear, or unknown geometries as has been a problem in the past with other flex fatigue testers. Again, as with the TFT, the strain is applied in balanced cycles. In one cycle on the BFT, a straight sample would be bent first to one side, returned to the straight position, bent to the other side, then returned to the straight position; the motion at all times both continuous and planar. For these fibers the maximum applied curvature, $(1/\rho)_{max}$, was ± 0.38, ± 0.30, or ± 0.26 mm^{-1} per cycle. For the 0.429-mm diameter monofilaments tested, the associated theoretical maximum applied surface strain, ϵ_{max}, was therefore ± 8.1, ± 6.4, or $\pm 5.6\%$, respectively, as

$$\epsilon_{max} = r(1/\rho)_{max}$$

where r is the fiber radius. Sample gauge length was fixed at 6.2 mm. For a fiber subjected to pure bending, curvature is uniform along the sample length.

Table III Relative Strength and Stiffness with Cycles of Torsional Fatigue

Cycles	Relative Strength	Expected Relative Stiffness	Actual Relative Stiffness
50,000	0.98	0.96	0.95
100,000	0.80	0.64	0.60
150,000	0.66	0.44	0.48

Strain is proportional to curvature; and the strain is at a maximum at the fiber surface in the plane of the bend, tensile at the outside of the bend, and compressive at the inside. Due to the balanced cycles of applied curvature with the BFT, for a given element in the fiber away from the neutral axis, the test is essentially a tension–compression fatigue test.

For the monofilaments fatigued in bending, the induced moment was seen to decay with time. The load response behavior for a typical nylon 66 monofilament at each of the three imposed strain levels is shown in Figure 6, where the induced bending moment has again been normalized with respect to the first recorded moment for the given sample. For many of these samples, the bending moment was seen to increase in value above the first recorded value during the early lifetime, and then drop in value as the crack formed and grew. The initial increase in stiffness is consistent with a strain-hardening mechanism often witnessed with the tensile fatigue of oriented fibers.[5,6]

Bending fatigue lifetime at each imposed strain level, defined arbitrarily as the number of cycles required to cause a 40% decay in bending moment, is plotted in S–N format in Figure 7. The data are summarized in Table IV; each lifetime value represents at least five samples. Here, as with torsional fatigue, there is no statistical difference ($\alpha = 0.01$) in bending fatigue lifetime between the low and high draw material. A least-squares fit to the combined low and high draw data yields a correlation coefficient of 0.89.

The failure of a nylon monofilament sample in bending fatigue is caused by the formation of one or more cracks that form and grow at an oblique angle to the fiber axis. A photograph of a typical crack formation in a fatigued nylon 66 monofilament is shown in Figure 8, where the plane of bending

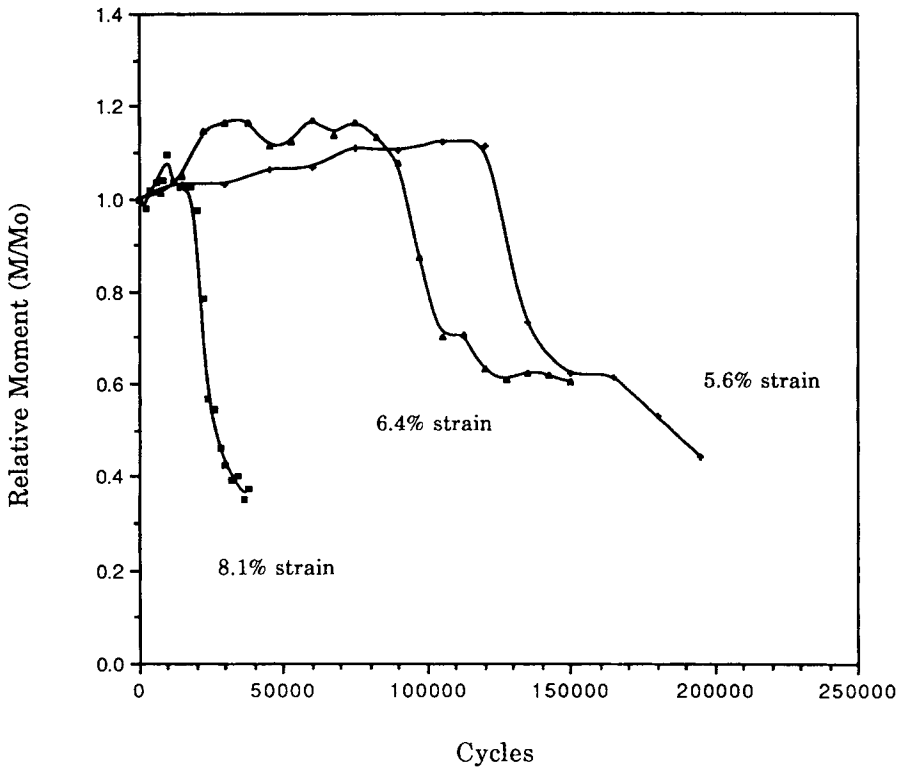

Figure 6 A typical response of nylon 66 monofilament to bending fatigue at each of three different imposed levels of maximum surface strain per cycle.

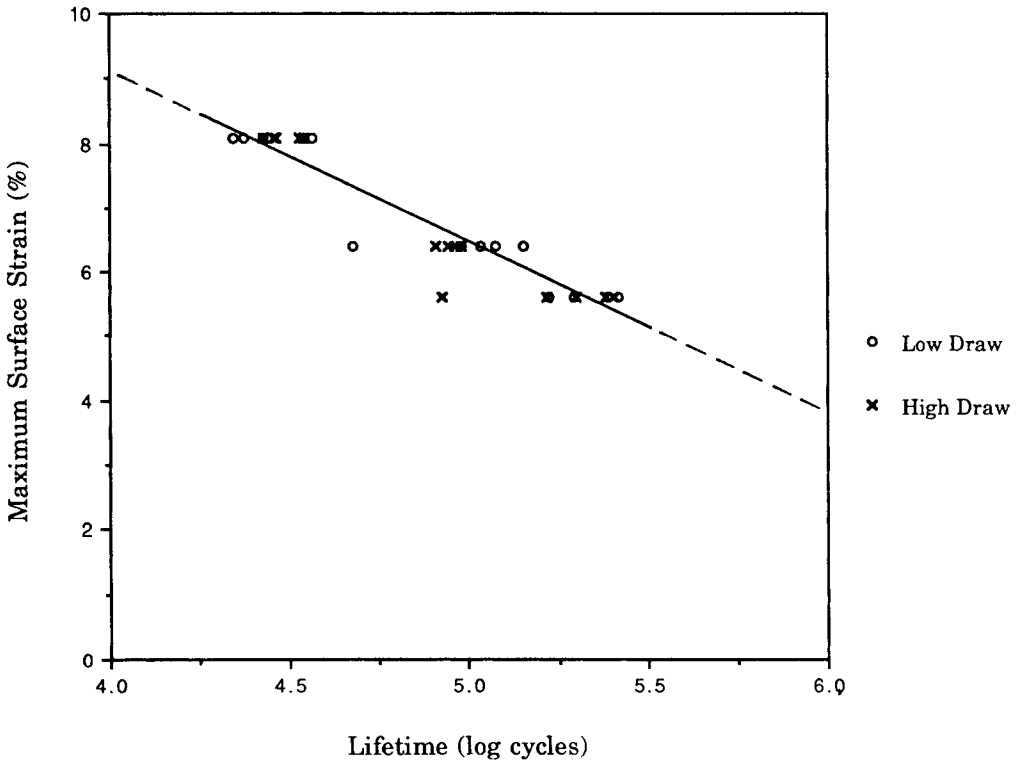

Figure 7 Bending fatigue S-N lifetime for nylon 66 monofilament.

Table IV Bending Fatigue Lifetimes at 60% Relative Moment

Maximum Curvature [mm^{-1}]	Maximum Surface Strain	Low Draw Mean Cycles [Thousands] (CV)	High Draw Mean Cycles [Thousands] (CV)
0.26	0.056	207.2 (21.8%)	188.9 (36.2%)
0.30	0.064	102.0 (34.3%)	88.8 (6.7%)
0.38	0.081	28.7 (22.9%)	30.6 (11.4%)

was in the plane of the page. The angle of the crack with respect to the fiber axis is independent of applied curvature or sample draw ratio and was measured to be about 20°. Similar oblique markings and cracks have been found in other oriented polymers as the result of flexing, bending, or axial compression.[7-15] The markings have been identified as kink bands and the oblique cracks usually associated with kink bands. A kink band is a localized buckling of an oriented structure as the result of axial compressive forces. The angle of a kink band or resulting crack with respect to the fiber axis appears to be polymer specific and evident only in oriented materials. For example, kink bands have been observed in compressed or bent polyethylene extrudate at angles of between 50 and 55°.[11-13] In Kevlar fibers, the kink band angles are between 50° and 60° and in PBZT fibers between 68° and 73°.[9,10] Although several workers have reported the observation of kink bands in nylon 66,[8,14,15] no values were reported for the angle of the kink bands. However, a kink band angle of 35° has been reported for nylon 6[7] and of 36°–43° for nylon 610.[8] For the fatigued nylon 66 fibers in this study, the angle of the kink band with respect to the fiber axis was measured to be between 30° and 35°. Scanning electron photomicrographs of kink bands in a fatigued nylon 66 monofilament are shown in Figure 9.

The apparent discrepancy between the angle of the kink bands (~30°) and the angle of the cracks

Figure 8 Typical crack formation in nylon 66 after bending fatigue.

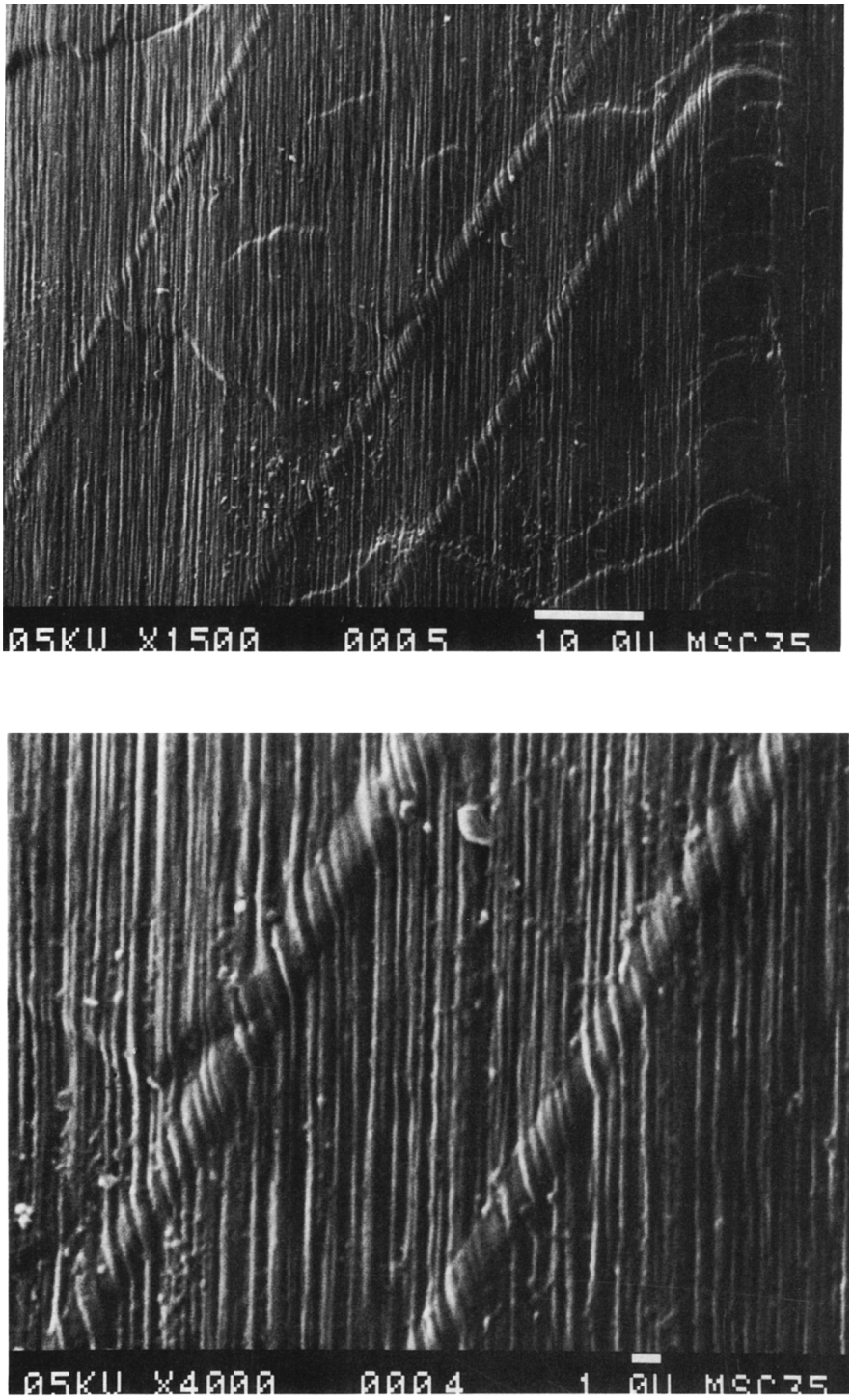

Figure 9 Scanning electron photomicrographs of kink bands in nylon 66 fibers fatigued in bending (↕ fiber axis).

(~20°) with respect to the fiber axis for these nylon 66 monofilaments is not well understood. Perhaps some plastic deformation during the cracking process disturbs the initial relative position; an axial plastic strain of only 9% could be responsible for a final crack angle of 20° from an initial kink band angle of 30°. Microscopic photographs of the crack edge do suggest local plastic deformation; there is a loss of surface definition and a pronounced bluntness to the crack edge.

Attempts have been made to model the fracture process in polymers as the viscous flow of molecules being the cause of the ultimate rupture. The original analysis by Tobolsky and Eyring[16] treated the flow in terms of reaction rate theory. This simple model has been used to successfully fit experimental data for synthetic fibers in either creep rupture or tensile fatigue at fixed stress amplitude.[17,18] For the nylon fibers tested here, the model suggests an activation energy of 25.2 and 26.6 kcal/mol for torsional and bending fatigue, respectively. In creep rupture, the required activation energies of 36 kcal/mol for the high draw and 42 kcal/mol for the low draw material are close to literature values for nylon fibers. Because of this discrepancy in calculated activation energies for the same fibers in different loading modes, the simple Tobolsky and Eyring model does not seem to be adequate to describe the fatigue behavior of synthetic fibers in modes other than uniaxial tension.

For nylon 66 monofilaments in each fatigue mode, the fatigue lifetime and failure mechanisms have been established. As the result of torsional fatigue, hydrogen bonds between adjacent microfibrils rupture and cause longitudinal cracks to form. The "soft" interface between microfibrils, as evidenced by the relatively low torsional stiffness of these oriented fibers, allows for easy axial slip of the microfibrils. In bending, the initial change in the fiber structure with fatigue is the formation of a kink band as the result of the applied compressive strains. Later, the tensile strains, which follow the applied compressive strains in each cycle, cause bond breakage within the weakened kink band region, culminating in macroscopic cracks. Although not discussed here, it was observed with these fibers that a surface roughening was capable of lowering the bending fatigue lifetime by an order of magnitude without appreciably changing the torsional fatigue lifetime of the monofilaments.

CONCLUSIONS

For these nylon 66 monofilaments in fatigue, multiple cycles of pure shear applied with respect to the fiber axis cause the formation of many longitudinal cracks, whereas multiple cycles of pure bending ultimately produce gross oblique cracks across the filaments. However, based on the limited study mentioned above, the fatigue lifetime of oriented materials in bending cannot be used to predict the fatigue lifetime in torsion, or vice versa. Further, for this group of nylon monofilaments, the level of orientation had no measurable effect on the fatigue lifetime in either bending or torsional fatigue. The range of draw was actually quite narrow (from 4.2× to 5.1×) but does represent the practical limit available with commercial processes.

With these testers, the fatigue behavior and lifetime of synthetic monofilaments can be easily characterized in either bending or torsion. The effects of such things as polymer type or processing conditions on fatigue behavior could be investigated. With these results, a better understanding can be developed of the failure of fibers in applications where the actual loading is a combination of these simple modes.

Funding for this research was provided by the Albany International Research Company and the work performed under Cornell University Agricultural Experiment Station Project NYS 329341.

REFERENCES

1. M. Toney, Ph.D. Dissertation, Cornell University (1991).
2. R. Meredith, *J. Text. Inst.*, **45,** T489 (1954).
3. B. C. Goswami and J. W. S. Hearle, *Tex. Res. J.*, **46,** 55 (1976).
4. A. K. Van der Vegt, *Rheo. Acta,* **2,** 17 (1962).
5. R. S. Chaunan and N. E. Dweltz, *Tex. Res. J.*, **55,** 658 (1985).
6. I. Narisawa, M. Ishikawa, and H. Ogawa, *J. Polym. Sci.*, **15,** 1055 (1977).
7. T. Ohta, *Sen-i-Gakk,* **45,** 337 (1989).
8. D. A. Zaukelies, *J. Appl. Phys.*, **33,** 2797 (1962).
9. S. J. DeTeresa, R. S. Porter, and R. J. Farris, *J. Mater. Sci.*, **23,** 1886 (1988).
10. W. Huh, S. Kumar, T. E. Helminiak, and W. W. Adams, *Proc. 48th ANTEC, Soc. Plastics Eng.*, 1245 (1990).
11. K. Imada, T. Yamamoto, K. Shigematsu, and M. Takayanagi, *J. Mater. Sci.*, **6,** 537 (1971).
12. A. G. Kolbeck and D. R. Uhlmann, *J. Polym. Sci.-Phys.*, **14,** 1257 (1976).
13. K. Shigematsu, K. Imada, and M. Takayanagi, *J. Polym. Sci.*, **13,** 73 (1975).
14. M. Miraftab, Ph.D. Dissertation, University of Manchester (1986).
15. J. W. S. Hearle, B. Lomas, W. D. Cooke, and I. J. Duerden, *Fibre Failure and Wear of Materials,* Ellis Horwood Ltd., Chichester, 1989.
16. A. Tobolsky and H. Eyring, *J. Chem. Phys.*, **11,** 125 (1943).
17. W. F. Busse, E. T. Lessig, D. L. Loughborough, and L. Larrick, *J. Appl. Phys.*, **13,** 715 (1942).
18. B. D. Coleman and A. G. Knox, *Text. Res. J.*, **27,** 393 (1957).

Received September 30, 1991
Accepted February 21, 1992